Engineering Failure Analysis 18 (2011) 1388–1394

Contents lists available at ScienceDirect

Engineering Failure Analysis

journal homepage: www.elsevier.com/locate/engfailanal

Short communication

Failure analysis of a car suspension system ball joint

E.A. Ossa [a,*], C.C. Palacio [b,1], M.A. Paniagua [a,2]

[a] Materials Engineering Research Group, Eafit University, Cra. 49 No. 7 sur 50, Medellin, Colombia
[b] Applied Electromagnetism Research Group, Eafit University, Cra. 49 No. 7 sur 50, Medellin, Colombia

ARTICLE INFO

Article history:
Received 9 November 2010
Received in revised form 10 March 2011
Accepted 23 March 2011
Available online 31 March 2011

Keywords:
Ball joint
Suspension system
Fatigue
Contact stress

1. Background

This study describes the analysis and investigation of the causes of the sudden failure of a MacPherson strut suspension system ball joint. The axis of the ball joint element showed a complete fracture which occurred midway between the top and bottom section changes of the element, as shown in Fig. 1. The failed ball joint element is shown in Fig. 1, along with a ball joint element not previously used, in order to show the height at which the fracture occurred in the element.

The aim of this study was to determine whether the failure was caused by defective materials, overload or deficient design of the element.

2. Experimental procedure

A fractographic inspection of the fractured surface of the element was initially performed using optical microscopy. After this inspection, samples were extracted to analyze the material microstructure and some of the fractographic features by means of Scanning Electron Microscopy (SEM). The microstructural analysis was performed in order to obtain information about previous thermo-mechanical treatments to the element. Optical Emission Spectroscopy (OES) was used to identify the chemical composition of the failed element. Vickers hardness was also measured on the failed element. It is worth noting that before any measurement was performed, any traces of grease and debris were removed from the element.

2.1. Fractographic study

Fig. 2 shows a macroscopic image of the fractured surface of the ball joint obtained by optical microscopy. Three different characteristic zones of the fracture are identified in the figure as zones A–C. Zones A and B indicate opposed zones where the

* Corresponding author. Tel.: +57 4 2619500; fax: +57 4 2664284.
E-mail addresses: eossa@eafit.edu.co (E.A. Ossa), cpalac12@eafit.edu.co (C.C. Palacio), mpaniag@eafit.edu.co (M.A. Paniagua).
[1] Tel.: +57 4 2619500; fax: +57 4 2664284.
[2] Tel.: +57 4 2619378; fax: +57 4 2664284.

1350-6307/$ - see front matter
doi:10.1016/j.engfailanal.2011.03.013

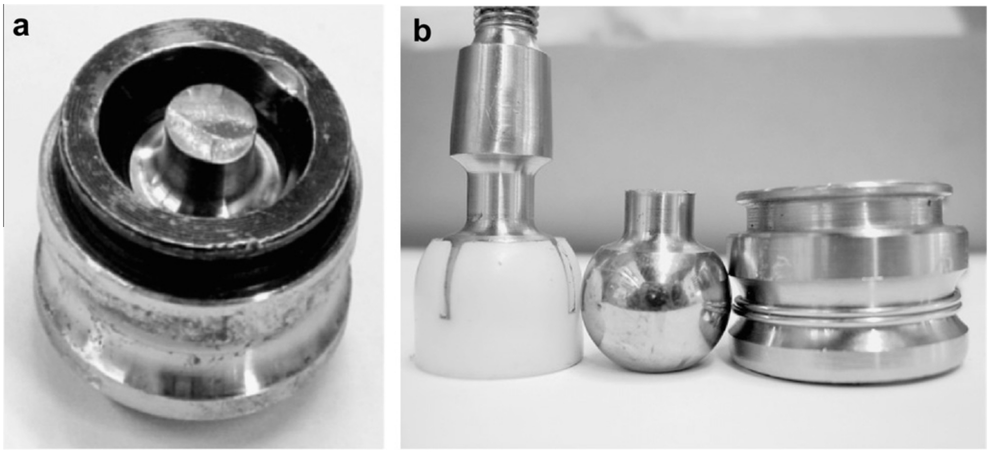

Fig. 1. Ball joint element. (a) Failed ball joint in the cage. (b) Failed and new ball joints out of the cage.

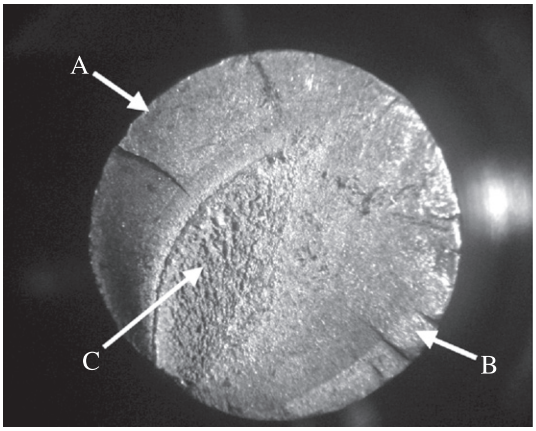

Fig. 2. Fracture surface of the failed ball joint.

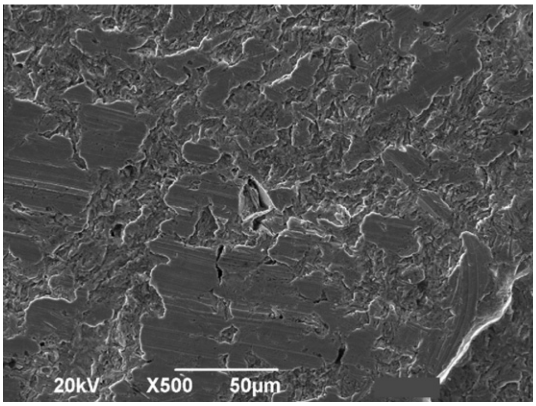

Fig. 3. SEM micrograph of fracture surface zone A.

crack growth started. These zones showed a smooth and curved appearance or beach marks. These zones are a clear indication of fatigue failure of the material. Furthermore, in zones A and B can be appreciated fracture features pointing towards the center of the fracture. These ratchet marks are typical of fracture on elements subjected to high stress concentrations. Zone C on the other hand shows a rough surface, indicating the final fracture zone of the element. This zone occupying

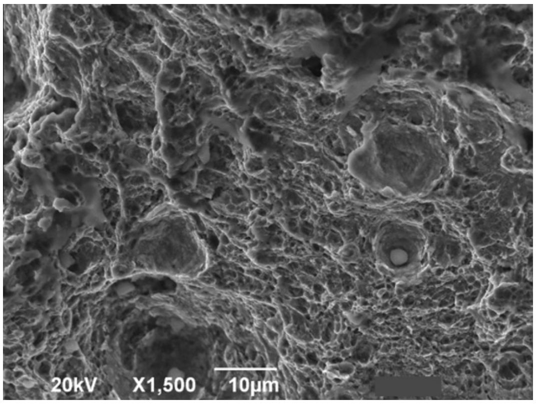

Fig. 4. SEM micrograph of fracture surface zone C.

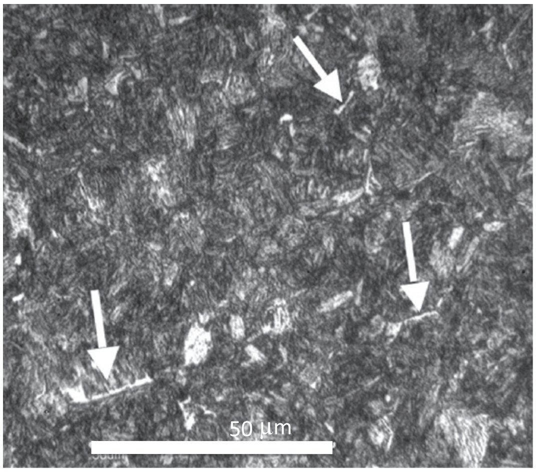

Fig. 5. Microstructure of the material. Etched with Nital 2%.

approximately one quarter of the cross section of the element. Fig. 3 shows a SEM micrograph of fracture zone A (see Fig. 2). There can be appreciated the smooth surface and the beach marks characteristics of fatigue crack propagation. Fig. 4 shows a SEM micrograph of zone C (see Fig. 2), where the micro-voids characteristic of final ductile fracture of the element can be appreciated.

2.2. Metallographic analysis

According to chemical composition analysis by OES, the ball joint was manufactured using an AISI-SAE 5140 steel. Fig. 5 shows the metallographic microstructure of the ball joint element. This micrograph shows a microstructure formed mainly by tempered martensite with acicular grains of ferrite on the grain boundaries (white grains indicated by arrows in Fig. 5). The presence of tempered martensite indicates that the material suffered a heat treatment of quenching and tempering. Despite the beneficial effect of increasing material toughness of acicular ferrite in low carbon steels [1–3], it has been found that acicular ferrite can decrease the fracture toughness and mechanical strength of heat treated steels when it appears on tempered martensite grain boundaries [4,5], as in the present case. The presence of acicular ferrite on grain boundaries can also induce a localized reduction on the hardness of the material, reducing the fatigue endurance limit, which along with the reduction on toughness can drastically reduce the life of the component. According to Murakami [6], the uniaxial fatigue strength σ_f can be related with the Vickers hardness H_v as:

$$\sigma_f = 1.6H_v \pm 0.1H_v. \quad (1)$$

The measured bulk Vickers hardness of the failed element was of $353H_v$. Therefore, using Eq. (1), the uniaxial fatigue strength of the material can be estimated as 565 MPa ± 35.3 MPa. Alsaran et al. [7,8] studied experimentally the effect of heat treatment on the properties of AISI-SAE 5140 steel used in the manufacture of suspension system ball joints, finding a fatigue

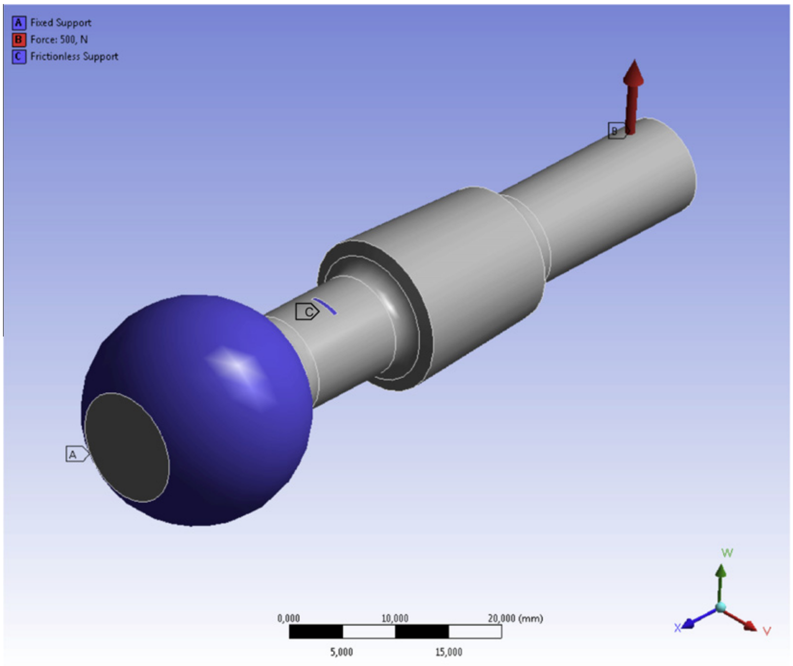

Fig. 6. Ball joint boundary and loading conditions used in the numerical analysis. A: Fixed support; B: Load 500 N; C: Fixed support.

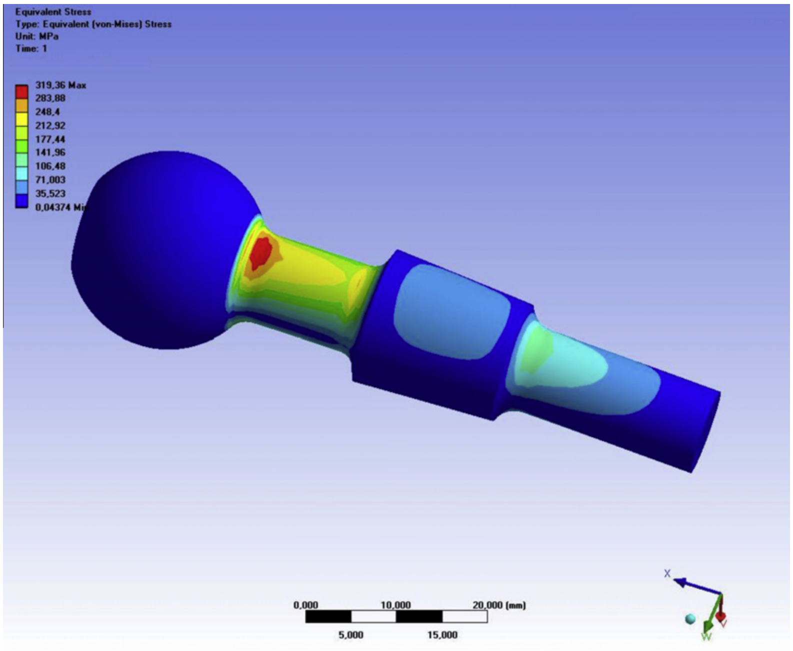

Fig. 7. Equivalent Von Mises stress distribution of the ball joint without contact support in C.

endurance limit of 416 MPa. As Alsaran's endurance limit is lower than the value found using Eq. (1), and was found experimentally, this value is then used as the bulk fatigue endurance limit of the failed ball joint element studied. Furthermore, Alsaran's value is more conservative.

The Vickers microhardness of the acicular ferrite on the tempered martensite grain boundaries was also measured, finding a mean value of $204H_v$. Using Murakami's Eq. (1), the endurance limit for the acicular ferrite approximates to

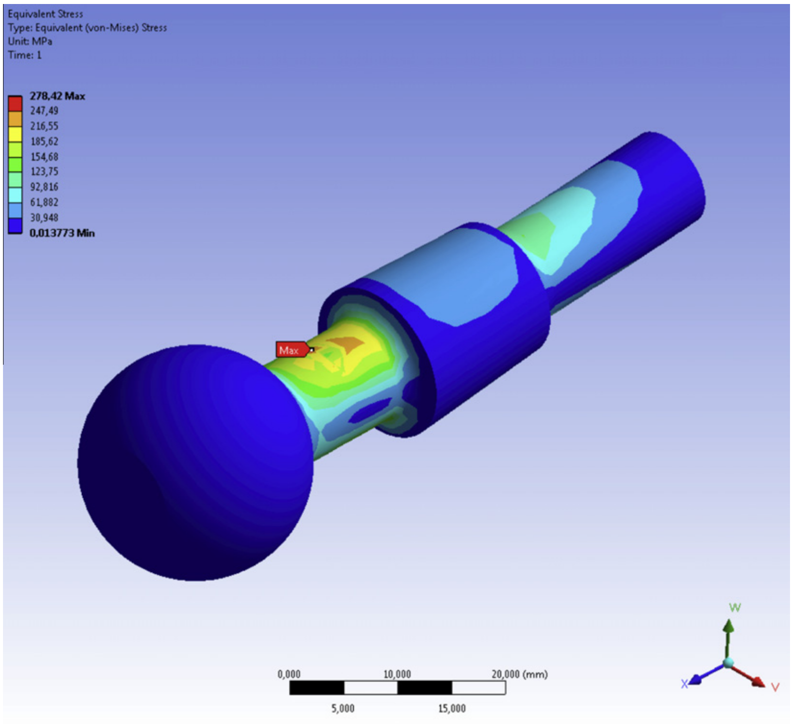

Fig. 8. Equivalent Von Mises stress distribution of the ball joint with contact support in C.

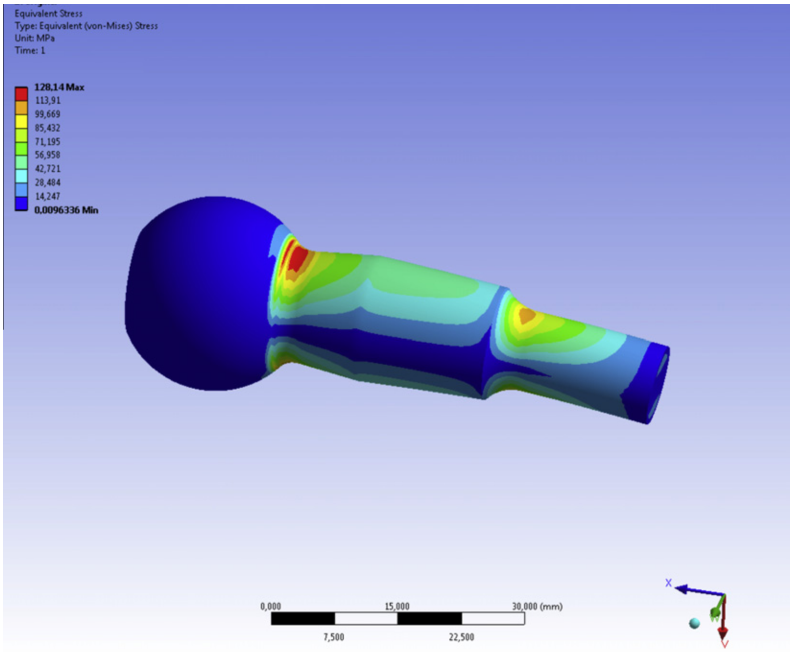

Fig. 9. Equivalent Von Mises stress distribution of the modified ball joint without contact support in C.

326 MPa ± 20.4 MPa. Despite the differences found on the endurance limit of the material by using Murakami's or Alsaran's approaches, it is evident that acicular ferrite reduces the endurance limit of the material in approximately 40%. This reduction on endurance limit is considered to be the cause of the fatigue crack initiation on the element, which was further enhanced by the contact stresses highlighted by the ratchet marks present on the fracture surface.

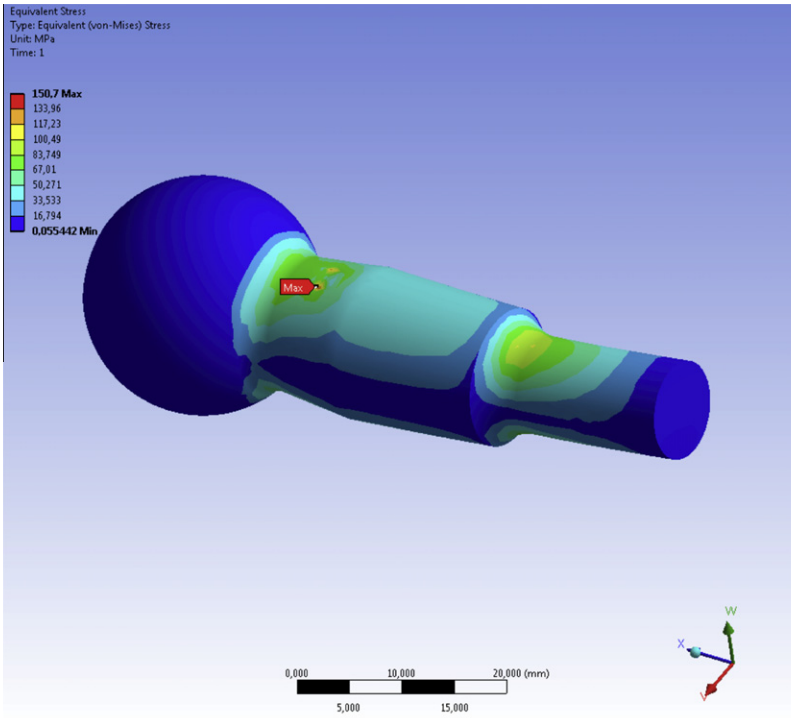

Fig. 10. Equivalent Von Mises stress distribution of the modified ball joint with contact support in C.

3. Finite Elements Analysis of the ball joint

Using Finite Elements Analysis (FEA) it is possible to find the locations of high stresses suffered by the analyzed element and their values. In this way it is feasible to draw specific conclusions on the causes and possible solutions to avoid the recurrence of these kind of failures. In this analysis the ball joint was geometrically modeled as shown in Fig. 6. The loading, boundary and contact conditions of the model are given as:

1. A fixed contact in zone A (ball), shown in blue[3] color in Fig. 6.
2. A lateral load B, assumed constant in this analysis to simplify the modeling, with a value of 500*N* and applied at the end of the element. This load value was used according to the experimental study of Ryu et al. [9], who found a value of lateral load of approximately 500*N* for a suspension system similar to the one studied here, so it is considered that this value of load represents a realistic estimate of the load applied to the element.
3. A lateral contact support patch in C, corresponding to the support of the axis of the ball joint element with its cage. This contact patch support was applied between the ball and the end of the element where the failure occurred (Fig. 1) with a rectangular shape as the real shape of contact of the ball joint element against its cage. The rectangle on the contact region had 1 mm thick by 3 mm long around the perimeter of the ball joint element.

The analysis and calculations of maximum stresses were performed both with and without the support C, in order to highlight the places of higher stresses in the element. The contact support between the axis of the element and its cage was modeled as frictionless because the failed element surfaces did not show any indications of fretting or wear suggesting friction between them.

The elements used in the FE mesh were hexagonal with a size of 2 mm. The mesh had a total of 3375 elements. The size of the elements and mesh were selected after performing series of analysis with the same loads and using different mesh sizes. These analyses showed that for elements smaller than 2 mm, the values of the stresses in the element varied considerably, reaching high values related with singularities caused by small elements. For elements bigger than 2 mm the results were not representative as the size of the elements were higher than the contact region.

Fig. 7 shows the stress distribution on the ball joint element without the contact support patch C in place. In this case the maximum stress was found on the section change between the ball and the axis. This stress reached a maximum value of 319 MPa approximately. On the other hand, Fig. 8 shows the stress distribution on the element including the contact support

[3] For interpretation of color in Figs. 6–10, the reader is referred to the web version of this article.

patch C in the calculations. In this case the maximum stress was found on the contact region between the axis of the element and its cage. This stress reached a maximum value of 278 MPa approximately, which is lower than the bulk fatigue endurance limit of this steel under normalized conditions, which reaches a value of 416 MPa [7]. However, this stress is close to the endurance limit found using Murakami's Eq. (1) for the acicular ferrite present in the grain boundaries of the material. Also note that the place where this stress is reached corresponds with the place where the fracture occurred in the ball joint element (see Fig. 1). The smooth beach marks accompanied by ratchet marks and a small final fracture zone (one quarter of the cross section of the element) confirm that the element suffered high stress low cycles fatigue conditions initiated at the acicular ferrite on the grain boundaries, followed by fatigue crack growth.

4. Conclusions and recommendations

The analysis showed that the ball joint suffered a fatigue induced fracture. The fracture initiated at the contact points between the ball joint element and its cage, where a stress concentration was created. Along with this stress concentrator, the presence of acicular ferrite on the tempered martensite grain boundaries reduced the fatigue endurance limit of the material on almost 40%, initiating cracks that grew with the application of loading cycles until the moment when the sudden failure of the element occurred.

The material used in the manufacture of the ball joint was appropriate for this kind of application. However, defective heat treating processes reduced the fatigue endurance limit of the material by formation of acicular ferrite on tempered martensite grain boundaries. Further, the reduction of the cross section on the ball joint element on the region of failure allows the formation of stress concentrators which further reduce the life of the element. Therefore, the causes of the failure of the ball joint are: (i) Defective heat treating process; and (ii) Defective geometric design of the element cross section.

In order to reduce the contact stresses on the ball joint element, a change on the geometric design of the element was proposed. In the proposed design, the cross section of the element was increased as sown in Fig. 9. This element was modeled using the same loading and boundary conditions employed for the failed element, as shown in Fig. 6. Fig. 9 shows the stress distribution on the proposed ball joint, being modeled without the cage support. In this case the maximum stresses were found on the section change between the ball and the axis of the element, with a maximum value of 128 MPa approximately. On the other hand, Fig. 10 shows the stress distribution of the proposed design considering the cage contact patch C. In this case the maximum stress was found on the cage contact, as expected, with a maximum stress value of 151 MPa, which is almost half the value reached in the same zone by the failed ball joint and well beyond the fatigue endurance limit of the material.

It is then suggested to modify the geometry of the ball joint to increase the loading section and reduce the contact stresses with the cage. It is also suggested to evaluate the heat treating processing conditions followed on the manufacture of the element to avoid the formation of acicular ferrite which further reduces the fatigue endurance limit of the element.

Acknowledgments

The authors wish to thank the technicians of the Materials Laboratory of the Eafit University for all their help and valuable discussions during the development of this study.

References

[1] He K, Edmonds DV. Formation of acicular ferrite and influence of vanadium alloying. Mater Sci Technol 2002;18:289–96.
[2] Bol'shakov VI, Laukhin DV, Sukhomlin GD, Kuksenko VI. Effect of heat treatment on formation of acicular ferrite and on the properties of low carbon microalloyed steels 10G2FB and 09G2S. Met Sci Heat Treat 2004;46(11–12):545–50.
[3] Mazancova E, Rucka Z, Mazanec K. Comparison of microfractographic behaviour of acicular ferrite and bainite and hydrogen cracking resistance. Arch Mater Sci 2007;28(1–4):95–9.
[4] Huang Z, Yao M. Effect of arrangement of acicular ferrite in a Widmanstatten microstructure on the fracture of mild steel. Mater Sci Eng: A 1989;119:211–7.
[5] E.A. Ossa, M. Paniagua, Failure analysis of a fastener system and its analytical prediction, SAMPE conference, Baltimore, MD, USA. 2009.
[6] Murakami Y. Metal fatigue: effects of small defects and non-metallic inclusions. Elsevier; 2002.
[7] Alsaran A, Karakan M, Celik A. The investigation of mechanical properties of ion-nitrided AISI 5140 low-alloy steel Materials Characterization. Mater Charact 2002;48:323–7.
[8] Bayrak M, Ozturk F, Demirezen M, Evis Z. Analysis of tempering treatment on material properties of DIN 41Cr4 and DIN 42CrMo4 steels. J Mater Eng Perform 2007;16(5):597–600.
[9] Ryu YI, Kang DO, Heo SJ, Yim HJ, Jeon JI. Development of analytical process to reduce side load in strut-type suspension. J Mech Sci Technol 2010;24:351–6.